



# Application of three-dimensional (3D) magnetic resonance (MR) Multi-Echo iN Steady-state Acquisition sequences in preoperative evaluation of lumbar disc herniation: a prospective study

Xuelin Pan<sup>1#</sup>, Yuting Wen<sup>1#</sup>, Kangkang Huang<sup>2</sup>, Jing Li<sup>2</sup>, Wanjiang Li<sup>1</sup>, Weijie Yan<sup>1</sup>, Deying Wen<sup>1</sup>, Miaoqi Zhang<sup>3</sup>, Shangxian Wang<sup>4</sup>, Xinyi Zhang<sup>5</sup>, Zhenlin Li<sup>1†</sup>, Xin Rong<sup>2†</sup>

<sup>1</sup>Department of Radiology, West China Hospital of Sichuan University, Chengdu, China; <sup>2</sup>Department of Orthopedics, West China Hospital of Sichuan University, Chengdu, China; <sup>3</sup>Department of Radiology, GE Healthcare, MR Research, Beijing, China; <sup>4</sup>Department of Radiology, The Johns Hopkins University, Baltimore, MD, USA; <sup>5</sup>West China School of Clinical Medicine of Sichuan University, Chengdu, China

*Contributions:* (I) Conception and design: Z Li, X Rong; (II) Administrative support: Z Li, X Rong, X Pan; (III) Provision of study materials or patients: K Huang, J Li; (IV) Collection and assembly of data: W Li, W Yan, D Wen; (V) Data analysis and interpretation: Y Wen, M Zhang; (VI) Manuscript writing: All authors; (VII) Final approval of manuscript: All authors.

<sup>#</sup>These authors contributed equally to this work as co-first authors.

<sup>†</sup>These two authors co-supervised this work.

*Correspondence to:* Prof. Zhenlin Li, MD. Department of Radiology, West China Hospital of Sichuan University, 37 Guoxue Alley, Chengdu 610041, China. Email: HX\_lizhenlin@126.com; Prof. Xin Rong, MD. Department of Orthopedics, West China Hospital of Sichuan University, 37 Guoxue Alley, Chengdu 610041, China. Email: rongxin@scu.edu.cn.

**Background:** Conventional spinal magnetic resonance imaging (MRI) cannot provide accurate diagnosis and surgical planning; thin-layer scanning can enhance the diagnostic efficacy. This study aimed to investigate the value of 3-dimensional (3D) magnetic resonance (MR) in preoperative evaluation of lumbar disc herniation, with a focus on the application of Multi-Echo iN Steady-state Acquisition (MENSA) sequence.

**Methods:** A total of 51 patients who underwent lumbar disc herniation surgery in West China Hospital of Sichuan University from June 2021 to December 2021 were prospectively enrolled. A cross-sectional study was conducted on those patients. The Cube group was scanned using 3D-FSE-Cube sequence, the Cube stir group was scanned using 3D-FSE-Cube Short Tau Inversion Recovery (STIR) sequence, and the MENSA group was scanned using MENSA sequence. Signal and noise values of nerve, herniated disc, ligamentum flavum (LF), and soft tissue were measured on the 3 groups. Signal-to-noise ratio (SNR) and contrast-to-noise ratio (CNR) were calculated. Objective scores were calculated by analysis of variance (ANOVA). Image quality was scored by a 5-point method. Friedman test was used to compare subjective scores, and Kappa test was used to evaluate the consistency of 2 readers' scores.

**Results:** The nerve root SNRs in the MENSA and Cube stir groups were higher than that in the Cube group ( $P < 0.01$ ), but there was no substantial statistical difference between the 2 groups. The herniated disc and LF SNRs of the MENSA group were greater than those of the Cube stir and Cube groups ( $P < 0.01$ ). Soft tissue SNR was greater in the MENSA group compared with the Cube stir group ( $P < 0.01$ ), which was greater than the SNR in the Cube group ( $P < 0.01$ ). The nerve root CNR of the Cube group ( $102.88 \pm 73.19$ ) was greater than that of the MENSA group ( $55.98 \pm 25.26$ ,  $P < 0.01$ ), which was higher than the CNR in the Cube Stir group ( $29.42 \pm 16.22$ ,  $P < 0.01$ ). The herniated disc CNR was higher in the MENSA and Cube groups than that in the Cube Stir group. The CNR of LF was greater in the MENSA group ( $37.71 \pm 16.87$ )

compared to the Cube group ( $29.76 \pm 25.73$ ,  $P=0.03$ ), which was greater than that in the Cube stir group ( $10.50 \pm 7.75$ ,  $P<0.01$ ). Among the subjective ratings of 2 reviewers, MENSA sequence scored highest in the qualitative measures of image quality. In the consistency test, the Kappa values of 2 readers for 3 groups of images were all greater than 0.73, indicating good consistency. The differences of subjective scores among all groups were statistically significant ( $P<0.05$ ). Overall, it was indicated that the consistency test results of the 2 readers were statistically significant and consistent. The MENSA group had the highest accuracy in diagnosing nerve compression. In addition, MENSA sequence ranked highest among the 3 sequences with 94.1% diagnostic accuracy.

**Conclusions:** The preoperative 3D MRI MENSA sequence can clearly depict the nerve roots and offer desirable contrast between the nerve roots, LF, bone, and intervertebral discs (IVDs). Patients with lumbar degeneration can effectively benefit from MENSA sequence since it provides useful imaging information to help understand disc herniation and compression of adjacent tissues when developing preoperative surgical strategies.

**Keywords:** 3-dimensional magnetic resonance (3D MR); Multi-Echo iN Steady-state Acquisition sequence (MENSA sequence); herniated disc; nerve root; preoperative assessment

Submitted Dec 25, 2023. Accepted for publication Jul 17, 2024. Published online Sep 13, 2024.

doi: 10.21037/qims-23-1834

View this article at: <https://dx.doi.org/10.21037/qims-23-1834>

## Introduction

Lumbar disc herniation is one of the most common diseases in the middle-aged and elderly population (1). Although 40–80% of patients with lumbar disc herniation respond well to conservative treatment, some patients continue to experience radiculopathy symptoms (2,3). To eliminate radiculopathy symptoms, thorough preoperative radiologic evaluations, such as X-ray, computed tomography (CT), and magnetic resonance imaging (MRI) (4,5), are essential prior to the operation. Among such imaging modalities, MRI has the advantage of imaging paraspinal and intraspinal soft tissues, including herniated disc, thecal sac, ligaments, and so on, without radiation (6).

Conventional spinal MRI includes sagittal T1-weighted and T2-weighted scans, and axial T2-weighted scans with approximately 2–4 mm layer thickness for diagnosis and surgical planning (7). However, a recent study found that such magnetic resonance (MR) sequences are generally acquired with large slice thickness, which may miss small lesions. Such diagnostic MRIs are therefore inadequate to provide sufficient information, resulting in false-positive or false-negative diagnoses (7,8). Furthermore, thick slices may cause discontinuity in nerve roots imaging, thus reducing image quality for nerve roots compression. Although an intuitive solution is reducing layer thickness, such an approach prolongs the scan time and increases the

possibility of motion artefacts.

Multi-Echo iN Steady-state Acquisition (MENSA) (9) is a novel acquisition technology based on 3-dimensional (3D) fast gradient echo sequence (FGRE) combined with spectral spatial RF (SSRF) to achieve selective water excitation. This method, which is mainly used for peripheral nerve and musculoskeletal imaging (10), improves the scanning efficiency also reduces the need for specific absorption rate (SAR).

Therefore, this study aimed to investigate the value of 3D MR examination in preoperative evaluation of lumbar disc herniation, and utilize MENSA to acquire images with higher resolution to identify herniated discs, hypertrophied ligaments, and compressed nerve roots, in a relatively short amount of scanning time. We present this article in accordance with the STROBE reporting checklist (available at <https://qims.amegroups.com/article/view/10.21037/qims-23-1834/rc>).

## Methods

### Study population

A total of 51 patients (17 males and 34 females, mean age  $61.10 \pm 11.36$  years, age range, 29–77 years) who were observed to have a herniated disc (detected by MR) and required surgery, were recruited between June 2021 to

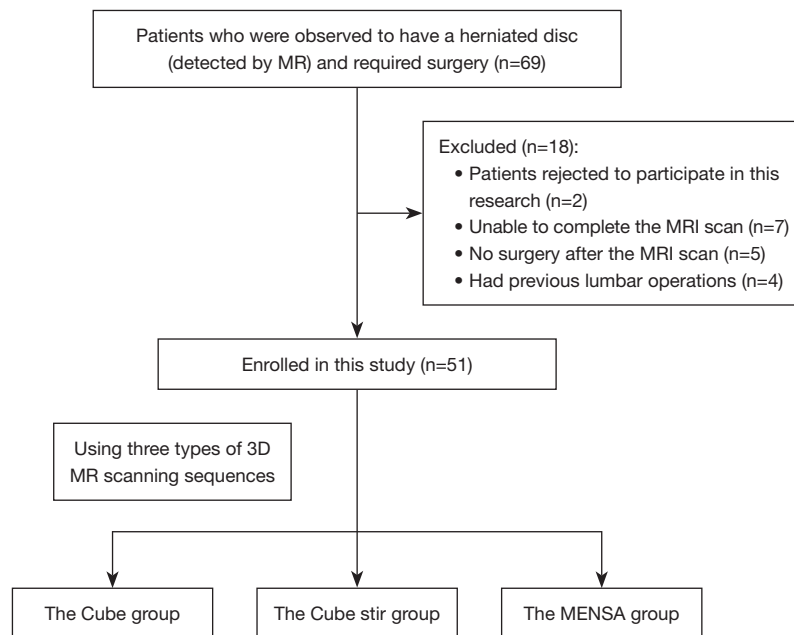


**Figure 1** Patients selection flow chart. MR, magnetic resonance; MRI, magnetic resonance imaging; 3D, 3-dimensional; MENSA, Multi-Echo iN Steady-state Acquisition.

December 2021 (*Figure 1*). A cross-sectional study was conducted on these patients.

This study was conducted in accordance with the Declaration of Helsinki (as revised in 2013). The study was approved by the Ethics Committee of West China Hospital of Sichuan University (approval No. 2021 Audit [1656] Number). Written informed consent was provided by every participant. Patients were recruited at the Orthopedics Outpatient Clinic. They were suspected of lumbar disc herniation and referred to the radiological department for further radiological evaluation. All the patients were selected according to the following inclusion criteria: (I) lumbar disc herniation confirmed by MRI scan; (II) had received surgery for lumbar disc herniation; and (III) no contraindications to MRI, including pregnancy or breast feeding, claustrophobia, and MRI-incompatible implants. The exclusion criteria were as follows: (I) refusal to participate in this research; (II) unable to complete the MRI scan; (III) no surgery after the MRI scan; and (IV) previous lumbar operations.

### Image acquisition

The lumbar MR scans were acquired using a 3.0T MRI scanner (Primer; GE Medical Systems, Milwaukee, WI,

USA) with a 60-channel spine coil. The regions of interest (ROIs) were manually measured in post-processing software, including segments with lesions from L1 vertebra to S1 vertebra. The ROIs were plotted for signal and standard deviation (SD) of background noise measurement, including nerve roots, intervertebral disc (IVD), ligamentum flavum (LF), bone, soft tissue, and air (*Figure 2*). The ROI areas were  $20 \pm 1 \text{ mm}^2$ . First, all lumbar spine MR examinations were performed on the basis of conventional lumbar spine MR scans. The common sequences were performed, including sagittal T2-weighted imaging (T2WI) Ideal-flex, sagittal T1-weighted imaging (T1WI) fast spin echo (FSE), and axial T2WI FSE. Then, the level of disc herniation was identified based on these sequences. Lastly, to evaluate herniated disc level, 3 additional sequences, including T2 cube, T2 cube stir, and MENSA, were performed. The Cube group was scanned using the 3D-FSE-Cube sequence, the Cube stir group was scanned using the 3D-FSE-Cube Short Tau Inversion Recovery (STIR), and the MENSA group was scanned using the MENSA sequence.

The scan was centered at the level of the herniated disc, covering the entire upper and lower vertebral bodies. The repetition time/echo time (TR/TE), flip angle, bandwidth, and matrix were different among the 3 sequences, whereas the field of view (FOV), slice thickness, and voxel volumes

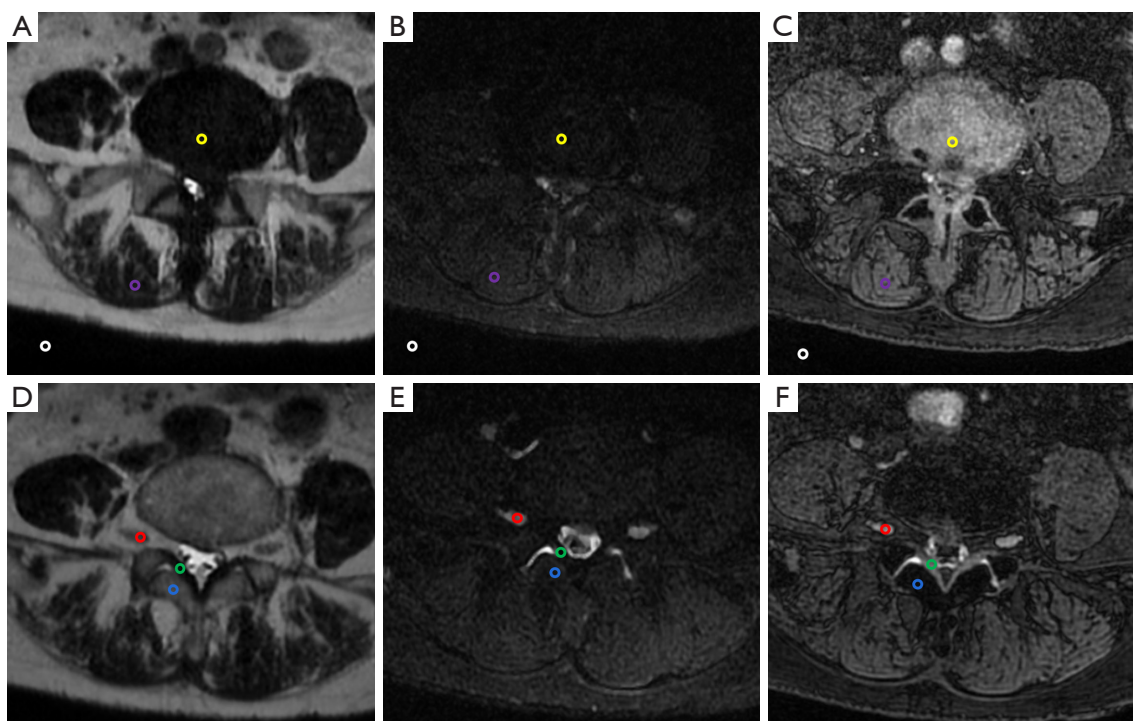


**Figure 2** The region of interest was plotted for signal and standard deviation of background noise measurement. (A,D) T2 cube sequence; (B,E) T2 cube stir sequence; (C,F) MENSAs sequence. Nerve roots (red), intervertebral disc (yellow), ligamentum flavum (green), bone (blue), soft tissue (purple), air (white). MENSAs, Multi-Echo iN Steady-state Acquisition.

remained identical (*Table 1*).

### Evaluation of the image quality

#### Quantitative assessment

The signal-to-noise ratio (SNR) and contrast-to-noise ratio (CNR) were used to evaluate the image quality. The SNR was calculated by dividing the mean signal by the mean SD of background noise:

$$SNR = SI_{ROI1} / SD_{ROI2} \quad [1]$$

and the CNR was calculated as the absolute value of the difference between the corresponding SNR values (11,12):

$$CNR = (SI_{ROI3} - SI_{ROI4}) / SD_{ROI2} \quad [2]$$

where ROI 1 represents nerve root, LF, bone, IVD, or soft tissue; ROI 2 represents air; ROI 3 represents nerves, IVD, or ligaments; ROI 4 represents soft tissue.

For T2 cube, T2 cube stir, or MENSAs, the same ROI at the level of the herniated disc, covering the entire upper

and lower vertebral bodies was selected. The ROI of signal and noise were in average 2 mm in diameter, respectively. For the SNR and CNR calculation, 6 points were chosen including nerve root, IVD, LF, bone, soft tissue, and air (*Figure 2*).

#### Qualitative assessment

A 5-point scale (*Table 2*) was used to evaluate the diagnostic value of the images acquired via 3 MRI sequences. The structure display sharpness was defined as the contrast between tissue structures, which can effectively display the herniated disc, nerve root, LF, bone, and soft tissue. The overall tissue contrast represented the inter-tissue signal contrast of herniated disc, nerve root, LF, bone, and soft tissue, and whether the tissue level is clear. The quality of reformats indicated the image quality of the coronal and sagittal images reoriented from the original axial images. Display of lesions (diagnostic certainty) represented the relative spatial relationships of spinal nerves, herniated discs, LF, and bone that are determined based on transverse or reconstructed images. For each sequence,

**Table 1** Acquisition parameters for MR sequences

Parameters	T2 cube	T2 cube stir	MENSA
TR/TE (ms)	3,021/120	3,031/90	15.6/5.2; 10.4
Flip angle (°)	90	90	35
Bandwidth (kHz)	62.5	62.5	31.25
Field of view (cm)	22.0×22.0	22.0×22.0	22.0×22.0
Matrix	320×256	384×288	272×272
Slice thickness (mm)	0.8	0.8	0.8
Voxel volume (mm <sup>3</sup> )	0.8×0.8×0.8	0.8×0.8×0.8	0.8×0.8×0.8
Scanning time (min)	4:58	4:53	4:55

3-slice averages in multiple planes were used to obtain 0.39×0.39 in-plane resolution and 0.8 mm sections. MR, magnetic resonance; MENSA, Multi-Echo iN Steady-state Acquisition; TR, repetition time; TE, echo time.

**Table 2** Ratings for the structure display sharpness, overall tissue contrast, quality of reformats, display of lesions

Rating	Structure display sharpness	Overall tissue contrast	Quality of reformats	Display of lesions (diagnostic certainty/ overall image impression)
1	Not visible/distinguishable	No contrast	Unable to reconstruct image	Not acceptable/no diagnostic value
2	Barely visible	Limited contrast	Poor quality	Very limited diagnostic value
3	Adequately visible	Certain contrast	Relatively good	Acceptable for most diagnoses
4	Good visibility	Clear	Good	Good for majority of diagnoses
5	Excellent visibility	Very clear	Very good	Optimal

both original and reconstructed images were provided for 2 senior readers (radiologists D.W. and W.Y., with 8 and 12 years of clinical experience, respectively) in random order. The 2 radiologists rated the images independently in 2 sessions at the interval of 4 weeks. Double-blind diagnosis was used to observe the nerve root compression in the 3 groups of images. The diagnostic accuracy of the 3 sequences was compared with the intraoperative results.

### Statistical analysis

All statistical analyses were performed using the software SPSS 21.0 (IBM Corp., Armonk, NY, USA). The SNR and CNR of the T2 cube, T2 cube stir, and MENSA groups were examined for normality and subjected to the Chi-squared test. One-way analysis of variance (ANOVA) was utilized to evaluate differences in SNR and CNR across the 3 groups, and least significant difference (LSD) post hoc tests were employed for between-group comparisons. Kappa test was used to evaluate the consistency of the 2 readers'

scores. Friedman test was used to compare the subjective scores of image quality. The scoring system of Fleiss *et al.* (13) was utilized in the analysis of our results (good >0.75, fair 0.4–0.75, poor <0.4). A P value <0.05 was deemed a statistically significant difference in this investigation, and all tests were 2-sided.

### Results

Of 53 patients examined in the study period, the data of 2 patients (both males, aged 63 and 67 years, respectively) was excluded due to incomplete scan or poor image quality. Therefore, 51 patients (mean age =61.10±11.36 years, 17 males and 34 females) ranging from 29 to 77 years old were included.

### Objective evaluation of image quality

The measurement data of the 3 groups were analyzed by variance, and the homogeneity of variance test was

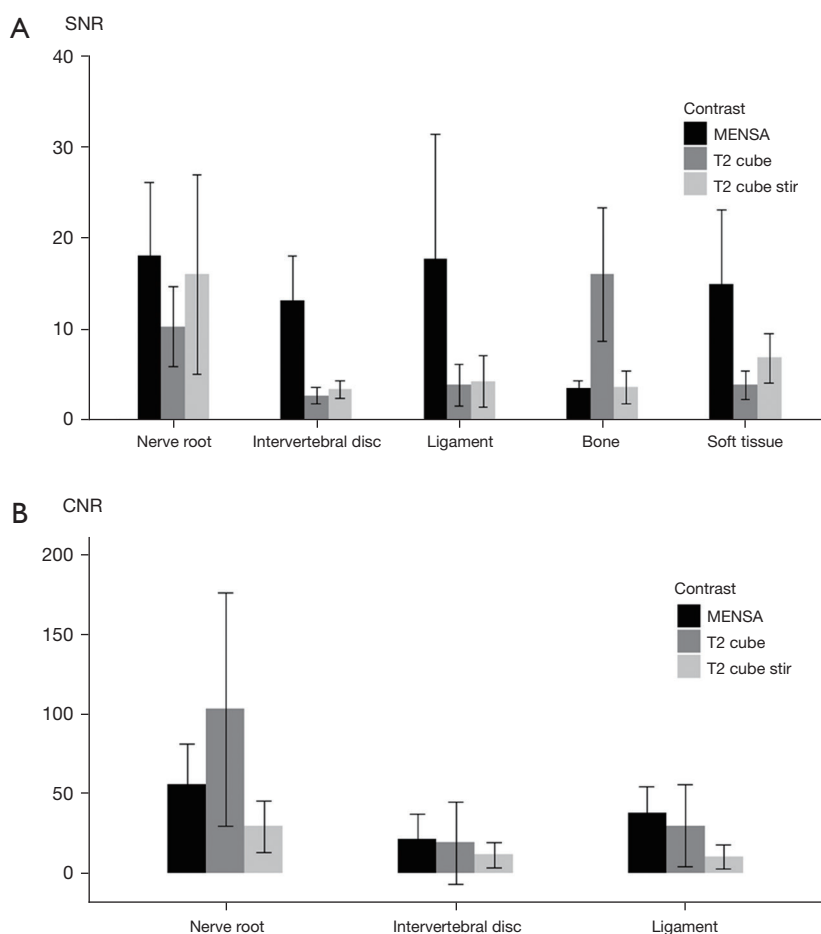


**Figure 3** SNR and CNR comparison among the 3 sequences for the quantitative measures. (A) MENSA had the statistically highest SNR, except for bone SNR. (B) MENSA had the statistically highest CNR, except for nerve root CNR. Paired *t*-test *P* values and rankings of subsequently lower. SNR, signal-to-noise ratio; CNR, contrast-to-noise ratio; MENSA, Multi-Echo iN Steady-state Acquisition.

performed first, which was consistent with normal distribution and homogeneity of variance ( $P < 0.05$ ).

### SNR

Figure 3 and Table 3 indicate that the nerve root SNR ( $18.00 \pm 8.07$ ) in the MENSA group did not statistically differ from the SNR ( $15.94 \pm 10.92$ ) in the Cube stir group ( $P = 0.2$ ), but they were both significantly higher than that ( $10.25 \pm 4.42$ ) in the Cube group ( $P < 0.01$ ). The IVD ( $13.03 \pm 4.95$ ) and LF ( $17.68 \pm 13.67$ ) SNRs of the MENSA group were significantly higher than those of the Cube stir ( $3.40 \pm 0.95$ ,  $4.22 \pm 2.84$ ) and Cube ( $2.68 \pm 0.92$ ,  $3.83 \pm 2.30$ ) groups ( $P < 0.01$ ). Soft tissue SNR ( $14.89 \pm 8.18$ ) in the MENSA group was significantly greater than that ( $6.80 \pm 2.72$ ) in the Cube stir group ( $P < 0.01$ ), whereas soft

tissue SNR in the Cube stir group was significantly greater than that ( $3.81 \pm 1.57$ ) in the Cube group ( $P < 0.01$ ).

### CNR

The nerve root CNR of the Cube group ( $102.88 \pm 73.19$ ) was significantly greater than the CNR of the MENSA group ( $55.98 \pm 25.26$ ,  $P < 0.01$ ), which was significantly higher than the CNR of the Cube Stir group ( $29.42 \pm 16.22$ ,  $P < 0.01$ ). The IVD CNRs were significantly higher in the MENSA and Cube groups than the CNR in the Cube Stir group. The CNR of LF was significantly greater in the MENSA group ( $37.71 \pm 16.87$ ) compared to the Cube group ( $29.76 \pm 25.73$ ,  $P = 0.03$ ), which was significantly greater than that in the Cube Stir group ( $10.50 \pm 7.75$ ,  $P < 0.01$ ).

**Table 3** Ranking of SNR and CNR between sequences (1 = highest, 3 = lowest)

Ranking	1	2	3
Nerve SNR	MENSA	Cube stir	Cube
P value	0.2	<0.01	–
Disc SNR	MENSA	Cube stir	Cube
P value	<0.01*	0.2	–
Ligament SNR	MENSA	Cube stir	Cube
P value	<0.01*	0.8	–
Bone SNR	Cube	Cube stir	Mensa
P value	0.8	<0.01	–
Soft tissue SNR	MENSA	Cube stir	Cube
P value	<0.01*	<0.01	–
Nerve CNR	Cube	Mensa	Cube stir
P value	<0.01*	<0.01	–
Disc CNR	MENSA	Cube	Cube stir
P value	0.5	0.03	–
Ligament CNR	MENSA	Cube	Cube stir
P value	0.03*	<0.01	–

MENSA had the highest nerve/intervertebral disc/ligament/soft tissue SNR and intervertebral disc/ligament CNR, but also the lowest bone SNR and the secondly highest nerve CNR. \*, the difference between this group and the other 2 groups are statistically significant ( $P<0.05$ ). SNR, signal-to-noise ratio; CNR, contrast-to-noise ratio; MENSA, Multi-Echo iN Steady-state Acquisition; Stir, Short Tau Inversion Recovery.

### Subjective evaluation of image quality

#### Diagnostic value

Two doctors, who were fellowship-trained, full-time musculoskeletal radiologists with 6 years of experience in MRI, were blinded to the surgical reports and unaware of the subjects' medical history. In the consistency test scores in 3 groups of images given by the 2 doctors, the Kappa values were all greater than 0.73, and most of them were greater than 0.75. The P values of the test were all less than 0.05. Such results indicate that the consistency test results of the 2 doctors were statistically significant and consistent (Table 4). There were statistically significant differences in the structure display sharpness, overall tissue contrast, quality of reformats and display of lesions, and the MENSA group performed better than the Cube group and the Cube Stir group across these features (all  $P<0.01$ ). MENSA

**Table 4** Average sequence rankings for qualitative measures of image quality for all reviewers combined (mean  $\pm$  standard deviation)

Item	T2 cube	T2 cube stir	MENSA	$\chi^2$	P
Structure display sharpness					
Reviewer 1	3.75 $\pm$ 0.48	4.06 $\pm$ 0.42*	4.80 $\pm$ 0.40*	73.12	<0.01
Reviewer 2	3.65 $\pm$ 0.48	3.96 $\pm$ 0.45*	4.84 $\pm$ 0.37*	77.6	<0.01
Kappa	0.824	0.756	0.731		
95% CI	0.665–0.983	0.540–0.972	0.484–0.978		
P value	<0.01	<0.01	<0.01		
Overall tissue contrast					
Reviewer 1	3.75 $\pm$ 0.48	3.53 $\pm$ 0.54	4.67 $\pm$ 0.48*	66.74	<0.01
Reviewer 2	3.75 $\pm$ 0.44	3.55 $\pm$ 0.54	4.67 $\pm$ 0.48*	68.6	<0.01
Kappa	0.806	0.924	0.824		
95% CI	0.628–0.984	0.820–1.000	0.657–0.991		
P value	<0.01	<0.01	<0.01		
Quality of reformats					
Reviewer 1	3.51 $\pm$ 0.54	3.61 $\pm$ 0.49	4.53 $\pm$ 0.50*	59.66	<0.01
Reviewer 2	3.41 $\pm$ 0.50	3.51 $\pm$ 0.50	4.59 $\pm$ 0.50*	66.06	<0.01
Kappa	0.845	0.803	0.881		
95% CI	0.704–0.986	0.642–0.964	0.752–1.0000		
P value	<0.01	<0.01	<0.01		
Display of lesions					
Reviewer 1	3.29 $\pm$ 0.46	3.29 $\pm$ 0.46	4.41 $\pm$ 0.50*	72.01	<0.01
Reviewer 2	3.29 $\pm$ 0.46	3.24 $\pm$ 0.428	4.43 $\pm$ 0.50*	75.08	<0.01
Kappa	0.811	0.749	0.799		
95% CI	0.635–0.987	0.543–0.854	0.632–0.966		
P value	<0.01	<0.01	<0.01		

\*, the difference between this group and the other two groups are statistically significant ( $P<0.05$ ). CI, confidence interval; Stir, Short Tau Inversion Recovery; MENSA, Multi-Echo iN Steady-state Acquisition.

sequence ranked highest among the 3 sequences with 94.1% diagnostic accuracy (Table 5). The pairwise comparison of the 3 groups of images had statistical significance (all  $P<0.01$ ).

### Discussion

This study compared image quality and diagnosing IVD pathology compression using MENSA, Cube, and Cube stir sequences. MENSA produced higher quality images, higher SNR, and higher CNR than the other 2 sequences.

**Table 5** Comparison of diagnostic accuracy of sequences with intraoperative outcome

Group	Positive predictor	Intraoperative outcome	Accuracy rate	95% CI	$\chi^2$	P value
T2 cube	27	51	52.9%*	38.7–67.1%	22.92	<0.01
T2 cube stir	39	51	76.5%*	64.9–88.1%		
MENSA	48	51	94.1%*	87.6–100%		

\*, indicates that the difference between this group and the other 2 groups are statistically significant ( $P < 0.05$ ). In pairwise comparison, the corrected P value is 0.016. CI, confidence interval; Stir, Short Tau Inversion Recovery; MENSA, Multi-Echo iN Steady-state Acquisition.

Several guidelines have suggested using MRI as an essential diagnostic tool, particularly for patients with radiculopathy or low back pain with red flag symptoms (14). The majority of scans were performed to detect possible lumbar degenerative illnesses, with an emphasis on disc herniations, neuroforaminal compression, and spinal stenosis. However, no standard for each specific components of a spine MRI scan has been defined. The European Society of Musculoskeletal Radiology (ESSR) provided general protocols, although it did not specify whether 2-dimensional (2D) or 3D sequences were preferred (15). Conventionally, preoperative MRI images of the lumbar spine only display a small portion of the nerve root in the spinal canal and the intervertebral foramen, which makes the structure and course of nerve roots difficult to capture. Thus, conventional preoperative 2D MRI sequences appear to be inadequate for nerve root compression detection.

In recent years, 3D MRI has been widely applied for suspected IVD pathology diagnosis (6). 3D MR neurography has been utilized to examine the whole nerve roots by enhancing the contrast between the nerve tissue and its surrounding tissues. It provides more detailed anatomical information and therefore assists to confirm diagnosis and surgical treatment plans. Pre-operative 3D MR examination accurately detects how the nerve roots are compressed, the location of the herniated disc, and its relation to the nerve roots and dura mater (16). Accurate pre-operative imaging is the prerequisite for precise diagnosis and pre-operative preparation. However, different MR sequences have shown varied image quality. Thus, it is imperative to identify which sequence is more suitable for detecting nerve compression due to lumbar degenerative changes.

This study was performed to compare the diagnostic values of 3 different 3D MR sequences (Cube, Cube stir, and MENSA) in detecting abnormalities of the nerve structure caused by lumbar degeneration. Cube is a fast-recovery 3D FSE technique with an extended echo-train

acquisition (XETA) that uses variable flip angles to constrain T2 decay throughout a lengthy echo train, allowing for the collection of T2WI with little blurring (17). Enabling STIR-produced pulse on cube can suppress the signal from tissues with a short T1 relaxation time comparable to fat, allowing imaging of peripheral nerves and the spine (18). The 3D-T2-Cube retains the benefits of 2D-FSE while addressing its shortcomings. However, the stir lipid suppression technique weakens the fat signal and reduces the SNR of other tissues, so that only the nerve roots are displayed more clearly, whereas the surrounding tissues are poorly displayed and cannot distinguish the nerve roots, IVDs, yellow ligaments, and other tissues well and cannot form a good inter-tissue contrast.

MENSA uses a similar technique to Double Echo Steady State (DESS) (11). MENSA generates free induction delay (FID)- and echo-like signals separately from steady-state free precession utilizing a prolonged and uneven readout gradient. It then combines the signals pixel by pixel, hence improving the SNR. MENSA's contrast is distinctive since it combines aspects of fast imaging with steady state precession (FISP)'s FID-signal and PSIF's echo-signal. Fluid that reflects T2/T1 weighting from the backward-running FISP (PSIF) echo signal is especially bright. Bone looks relatively dark due to T2 dephasing from trabeculae, revealing the susceptibility sensitivity of the FISP/FID component (19,20). Using MENSA for neuroimaging provides more resistance to blood flow's high signal interference than other conventional sequences. In addition, MENSA reduced the effects of fat distortion and nerve distortion in conventional diffusion-weighted imaging (DWI) and diffusion tensor imaging (DTI) scans and produced thin, noninvasive MRI pictures of nerves and ligaments. MENSA provides a high SNR for not only nerve roots, but also for IVD, LF, and soft tissue (10). The enhanced contrast between tissues produced by MENSA enables more detailed visualization of lesions and its surrounding structures. Furthermore, MENSA sequence could be reconstructed in 3D, providing



a clear illustration of the compression of nerve roots and IVDs. The high spatial resolution and isovolumetric acquisition without gaps enables a full 360° angulation along anatomical structures such as the nerve roots (21) and are particularly useful in evaluating complex anatomy as in IVD herniation (22).

This study validates theoretical advantages of the MENSA sequence over conventional Cube and Cube stir sequences mentioned above. Our data demonstrated that MENSA sequence has a superior SNR to the Cube and Cube stir sequences in nerve, IVD, LF, and soft tissue. Also, the MENSA sequence has superior CNR of LF and IVD compared to soft tissue. Besides, the MENSA sequence had considerably higher subjective scores for IVD, nerve root, LF, bone, soft tissue display clarity, overall tissue contrast, quality of reformats, and relevance of disc herniation than the other 2 sequences.

Although the SNR of bone in the MENSA sequence was lower than that in Cube and Cube stir, this was determined by the characteristics of the MENSA sequence itself. Bone of the MENSA sequence looks relatively dark due to T2 dephasing from trabeculae, revealing the susceptibility sensitivity of the FISP/FID component. The CNR of nerve root in the MENSA group was lower than that in the Cube group, because of the calculation of CNR, the reference tissue was the signal value of soft tissue. This study chooses soft tissue as the background reference. In the MENSA sequence, soft tissue showed a slightly higher signal, which was not much different from the signal of nerve root. In the Cube group, the soft tissue showed slightly lower signals, and the signals were quite different from those of nerve root. However, the nerve root is adjacent to the IVD and bone, so even if the CNR of MENSA is smaller than that of the muscle, it will not affect the contrast between the nerve root and the surrounding tissue.

Therefore, according to the comprehensive judgment of SNR, CNR, diagnostic accuracy, and subjective image score, the MENSA sequence has obvious advantages over the Cube and Cube stir sequences in nerve root display and comparison between nerve root and surrounding tissue.

This study has several limitations. First, due to the absence of a prior sample size estimation and relatively small sample size, the present results may not be conclusive due to insufficient power. Second, the images may have had significant motion artefacts when scanning period was prolonged. This study verified that MENSA sequence can clearly display nerve roots, herniated disc, and other structures, and only MENSA sequence can be scanned

in clinical examination to reduce the examination time of patients. Third, MENSA sequence needs to be used in conjunction with conventional MR scan; it cannot be used without standard turbo spin-echo (TSE) images.

## Conclusions

Preoperative 3D MRI MENSA sequence is able to effectively depict the nerve roots and offers desirable contrast between the nerve roots, LF, bone, and IVDs. It benefits patients with lumbar degeneration since it provides more detailed tissue information, therefore enables more solid understanding of disc herniation and compression of adjacent tissues when developing preoperative surgical strategies.

## Acknowledgments

*Funding:* This work was supported by 1·3·5 Project for Disciplines of Excellence, West China Hospital, Sichuan University (No. ZYGD23024), and the Key R&D Projects of Sichuan Science and Technology (No. 2023YFG0126).

## Footnote

*Reporting Checklist:* The authors have completed the STROBE reporting checklist. Available at <https://qims.amegroups.com/article/view/10.21037/qims-23-1834/rc>

*Conflicts of Interest:* All authors have completed the ICMJE uniform disclosure form (available at <https://qims.amegroups.com/article/view/10.21037/qims-23-1834/coif>). The authors have no conflicts of interest to declare.

*Ethical Statement:* The authors are accountable for all aspects of the work in ensuring that questions related to the accuracy or integrity of any part of the work are appropriately investigated and resolved. This study was conducted in accordance with the Declaration of Helsinki (as revised in 2013). The study was approved by the Ethics Committee of West China Hospital of Sichuan University (approval No. 2021 Audit [1656] Number). Written informed consent was provided by every participant.

*Open Access Statement:* This is an Open Access article distributed in accordance with the Creative Commons Attribution-NonCommercial-NoDerivs 4.0 International License (CC BY-NC-ND 4.0), which permits the non-

commercial replication and distribution of the article with the strict proviso that no changes or edits are made and the original work is properly cited (including links to both the formal publication through the relevant DOI and the license). See: <https://creativecommons.org/licenses/by-nc-nd/4.0/>.

## References

- Hoy D, Brooks P, Blyth F, Buchbinder R. The Epidemiology of low back pain. *Best Pract Res Clin Rheumatol* 2010;24:769-81.
- Thoomes EJ, Scholten-Peeters GG, de Boer AJ, Olsthoorn RA, Verkerk K, Lin C, Verhagen AP. Lack of uniform diagnostic criteria for cervical radiculopathy in conservative intervention studies: a systematic review. *Eur Spine J* 2012;21:1459-70.
- Jin C, Li H, Li X, Wang M, Liu C, Guo J, Yang J. Temporary Hearing Threshold Shift in Healthy Volunteers with Hearing Protection Caused by Acoustic Noise Exposure during 3-T Multisequence MR Neuroimaging. *Radiology* 2018;286:602-8.
- Bell GR, Ross JS. Diagnosis of nerve root compression. Myelography, computed tomography, and MRI. *Orthop Clin North Am* 1992;23:405-19.
- Brown BM, Schwartz RH, Frank E, Blank NK. Preoperative evaluation of cervical radiculopathy and myelopathy by surface-coil MR imaging. *AJR Am J Roentgenol* 1988;151:1205-12.
- Sung J, Jee WH, Jung JY, Jang J, Kim JS, Kim YH, Ha KY. Diagnosis of Nerve Root Compromise of the Lumbar Spine: Evaluation of the Performance of Three-dimensional Isotropic T2-weighted Turbo Spin-Echo SPACE Sequence at 3T. *Korean J Radiol* 2017;18:249-59.
- Hosseini J, Fariborz F, Mehrnaz R, Babak R. Evaluation of diagnostic value and T2-weighted three-dimensional isotropic turbo spin-echo (3D-SPACE) image quality in comparison with T2-weighted two-dimensional turbo spin-echo (2D-TSE) sequences in lumbar spine MR imaging. *Eur J Radiol Open* 2019;6:36-41.
- Lee S, Jee WH, Jung JY, Lee SY, Ryu KS, Ha KY. MRI of the lumbar spine: comparison of 3D isotropic turbo spin-echo SPACE sequence versus conventional 2D sequences at 3.0 T. *Acta Radiol* 2015;56:174-81.
- Hardy PA, Recht MP, Piraino D, Thomasson D. Optimization of a dual echo in the steady state (DESS) free-precession sequence for imaging cartilage. *J Magn Reson Imaging* 1996;6:329-35.
- Eckstein F, Hudelmaier M, Wirth W, Kiefer B, Jackson R, Yu J, Eaton CB, Schneider E. Double echo steady state magnetic resonance imaging of knee articular cartilage at 3 Tesla: a pilot study for the Osteoarthritis Initiative. *Ann Rheum Dis* 2006;65:433-41.
- Chen CA, Kijowski R, Shapiro LM, Tuite MJ, Davis KW, Klaers JL, Block WF, Reeder SB, Gold GE. Cartilage morphology at 3.0T: assessment of three-dimensional magnetic resonance imaging techniques. *J Magn Reson Imaging* 2010;32:173-83.
- Wu R, Hori M, Onishi H, Nakamoto A, Fukui H, Ota T, Nishida T, Enchi Y, Satoh K, Tomiyama N. Effects of reconstruction technique on the quality of abdominal CT angiography: A comparison between forward projected model-based iterative reconstruction solution (FIRST) and conventional reconstruction methods. *Eur J Radiol* 2018;106:100-5.
- Fleiss JL, Levin B, Paik MC. *Statistical methods for rates and proportions* (3rd ed.). Hoboken, NJ: John Wiley & Sons, 2003.
- Pillastrini P, Gardenghi I, Bonetti F, Capra F, Guccione A, Mugnai R, Violante FS. An updated overview of clinical guidelines for chronic low back pain management in primary care. *Joint Bone Spine* 2012;79:176-85.
- European Society of Skeletal Radiology. Guidelines for MRI imaging of Sports Injuries. Available online: <https://essr.org/content-essr/uploads/2016/10/ESSR-MRI-Protocols-Spine.pdf>. Accessed May 31, 2018.
- Hu S, Li Y, Hou B, Zhang Y, Liu WV, Wu G, Li X. Multi-echo in steady-state acquisition improves MRI image quality and lumbosacral radiculopathy diagnosis efficacy compared with T2 fast spin-echo sequence. *Neuroradiology* 2023;65:969-77.
- Busse RF, Hariharan H, Vu A, Brittain JH. Fast spin echo sequences with very long echo trains: design of variable refocusing flip angle schedules and generation of clinical T2 contrast. *Magn Reson Med* 2006;55:1030-7.
- Bowen BC, Pattany PM, Saraf-Lavi E, Maravilla KR. The brachial plexus: normal anatomy, pathology, and MR imaging. *Neuroimaging Clin N Am* 2004;14:59-85, vii-iii.
- Bruder H, Fischer H, Graumann R, Deimling M. A new steady-state imaging sequence for simultaneous acquisition of two MR images with clearly different contrasts. *Magn Reson Med* 1988;7:35-42.
- Thakkar RS, Flammang AJ, Chhabra A, Padua A, Carrino JA. 3T MR imaging of cartilage using 3D dual echo steady state (DESS). *MAGNETOM Flash* 2011;3:33-6.
- Kijowski R, Gold GE. Routine 3D magnetic resonance

imaging of joints. *J Magn Reson Imaging* 2011;33:758-71.

22. Tins B, Cassar-Pullicino V, Haddaway M, Nachtrab U. Three-dimensional sampling perfection with application-

optimised contrasts using a different flip angle evolutions sequence for routine imaging of the spine: preliminary experience. *Br J Radiol* 2012;85:e480-9.

**Cite this article as:** Pan X, Wen Y, Huang K, Li J, Li W, Yan W, Wen D, Zhang M, Wang S, Zhang X, Li Z, Rong X. Application of three-dimensional (3D) magnetic resonance (MR) Multi-Echo iN Steady-state Acquisition sequences in preoperative evaluation of lumbar disc herniation: a prospective study. *Quant Imaging Med Surg* 2024;14(10):7540-7550. doi: 10.21037/qims-23-1834